

Tracking and Vibration Control of Flexible Robots Using Shape Memory Alloys

Shuzhi Sam Ge, *Fellow, IEEE*, Keng Peng Tee, *Student Member, IEEE*, Ivan E. Vahhi, and Francis E. H. Tay

Abstract—This paper considers the tracking control problem for flexible robots with active vibration suppression by shape memory alloys (SMAs). With a singular perturbation technique, the flexible modes and joint angles are modeled as fast and slow variables, respectively. The fast subsystem comprising the nonlinear SMA dynamics is obtained in a strict feedback form feasible for the backstepping design. The SMA actuators are configured in redundant pairs for an active suppression of vibrations. For the slow subsystem, asymptotically stable tracking is ensured, while for the fast subsystem, uniform exponential stability is guaranteed. By invoking Tikhonov's theorem, it is shown that the error arising from the nonideal time-scale separation in the singular perturbation model is small. Simulation demonstrates the effectiveness of the proposed control.

Index Terms—Backstepping, flexible link, shape memory alloys (SMAs), singular perturbation, vibration.

I. INTRODUCTION

FLEXIBLE robots are governed by the partial differential equations (PDEs), which attribute infinite dimensionality to the system. As a simplified approach, truncated models, based on either the finite element method (FEM) or the assumed modes method (AMM), are often used, and a number of means have been undertaken to improve the performance of the flexible systems [1]–[3]. There are also a few results on control design based directly on the PDEs [4]–[6], which avoid problems such as controller/observer spillover that results from the use of the truncated models.

One method of dealing with the tracking control problem of the flexible robots is to employ the singular perturbation technique [3], [7], [8]. Since the joint motion is relatively slow as compared to the link vibrations, the former is treated as “slow” dynamics and the latter as “fast” dynamics. For the “slow” joint motion dynamics, well-established control schemes designed for rigid manipulators can be used, such as computed torque control, robust control, adaptive control, and neural network control. As for the fast subsystem, the control objective is one of stabilizing the origin, and it is important for the control action to be sufficiently fast for an effective stabilization.

Besides singular perturbation technique, energy-based robust control (EBRC) was proposed for the multi link flexible robots, wherein a robust term associated with the vibration variables is augmented to the traditional collocated base proportional-derivative (PD) control law [9]. This innovative method exploits a fundamental energy relationship of the system and does not require any information on the system dynamics, thereby avoiding limitations of the model-based methods, including controller/observer spillover in the truncated models, as well as complexity of analysis in the PDE-based models. In [10], the energy-based approach was extended to the multi-link flexible robots with redundant piezoelectric actuators.

Shape memory alloys (SMAs) have been widely employed as actuators and sensors in applications including smart structures, biomedical devices, and robotics. When heated above the transformation temperature, the SMAs undergo a change in the crystal structure, thereby generating large forces that can be used to actuate the control systems. However, due to the inherently nonlinear and complex dynamic behavior of the SMA actuators, it is generally difficult to design a controller that guarantees a closed loop stability within the performance bounds. Linear controllers, notably PID variants, have been widely investigated for the control of the SMA actuators [11], [12]. In the last decade, there has been a growing interest in the use of the nonlinear control techniques for the SMA systems, and a wide variety of control strategies has been proposed, including model-based feedback linearization [13], [14], variable structure control [15], time-delay control [16], and neural networks [17]. In [18], a model-based backstepping control was employed for the global asymptotic stabilization of a rotary SMA-actuated robotic arm. For an active vibration control of *static* structures, the SMAs have been found to be suitable candidates [19], [20].

There are comparative merits and demerits of the SMA actuators with respect to the piezoelectric actuators. On the one hand, the SMA actuators are capable of producing large forces, withstanding large stresses, and recovering large strains. This is unlike the piezoelectric actuators, which are brittle, and when subjected to large stresses, can become depolarized and ineffective. On the other hand, SMA actuators are well known to have a slow speed of response, and thus, lose effectiveness at high frequencies of vibration. Piezoelectric actuators, however, can operate at frequencies of the order of 10 kHz. The slow response of the SMA can be partially circumvented by reducing the size of the actuators to increase the rate of heat transfer, although the associated decrease in the force production needs to be accommodated. Furthermore, the rate of response may be accelerated by employing, wherever

Manuscript received August 26, 2005; revised July 11, 2006. Recommended by Technical Editor C. Cecati.

S. S. Ge and K. P. Tee are with the Department of Electrical and Computer Engineering, National University of Singapore, 117576 Singapore (e-mail: eleges@nus.edu.sg; kptee@nus.edu.sg).

I. E. Vahhi is with the Department of Material Study and Technology, St. Petersburg State Polytechnic University, 195251 St. Petersburg, Russia (e-mail: vahhi@iv4817.spb.edu).

F. E. H. Tay is with the Department of Mechanical Engineering, National University of Singapore, 117576 Singapore (e-mail: mpetayeh@nus.edu.sg).

Digital Object Identifier 10.1109/TMECH.2006.886242

possible, more efficient modes of cooling, such as forced convection and/or use of coolants. In general, the SMA-based controls, proposed in this paper, are more suitable for relatively large robots that involve large forces, large displacements, and low frequencies of vibrations, while piezoelectric-based control [8], [10] are suitable for smaller robots with high-frequency vibrations.

Motivated by the effectiveness of the SMAs in the active vibration control of *static structures*, we conduct a theoretical and numerical investigation of the use of the SMAs in suppressing the vibrations of a *flexible robot* that is dynamically tracking a desired trajectory. We adopt a macroscopic phenomenological model of the SMA based on [21]–[23], which consider martensite as an internal state of the constitutive model and account for the thermodynamic effects on the internal state.

For the control of the SMA-based flexible robot system, singular perturbation technique is used, in which the flexible modes and the joint variables are modeled as fast and slow variables, respectively. The slow subsystem is controlled by the joint motor torques, while the fast subsystem is actively controlled by the SMA actuators that span the length of the flexible links. By a suitable state transformation, the fast subsystem is rendered into an affine strict-feedback form suitable for backstepping. The computed torque controller for the slow subsystem ensures asymptotically stable trajectory tracking while the backstepping controller for the fast subsystem guarantees uniform exponential stability. Using Tikhonov's theorem, we show that the discrepancy between the actual states and those modeled using singular perturbation is small.

The methods and the results presented in this paper are different from the existing works on the vibration suppression of the flexible link robots [5], [6], [8]–[10]. These works were based on the distributed-parameter system models [5], [6], as well as model-free energy-based approach [9], [10], which are fundamentally different from the approach undertaken in this paper. Although singular perturbation technique used in this paper was found in [8], the latter involved neural networks, and the fast subsystem was a linear system. In this paper, the fast subsystem is nonlinear and involves the complex SMA dynamics. Additionally, the SMA actuators are unidirectional and need to be coordinated in antagonist pairs, as developed in this paper, unlike the piezoelectric actuators that are bi-directional and relatively simpler to deal with.

II. PROBLEM FORMULATION AND PRELIMINARIES

A. Sma Actuator Dynamics

Consider the SMA actuator configuration on a flexible link, as shown in Fig. 1. The SMA actuators are wires that act in pairs to provide a bidirectional control. Throughout this paper, we use the notations $(\cdot)^+$ and $(\cdot)^-$ to denote the terms pertaining to the SMA actuators in an antagonist pair, i.e., the actuators tend to counteract. For consistency, all actuators on one side of the link will be labeled $(\cdot)^+$, while those on the opposite side will be labeled $(\cdot)^-$. Note that in the given configuration of Fig. 1, each pair of the agonist–antagonist SMA wires act at the same point on the link.

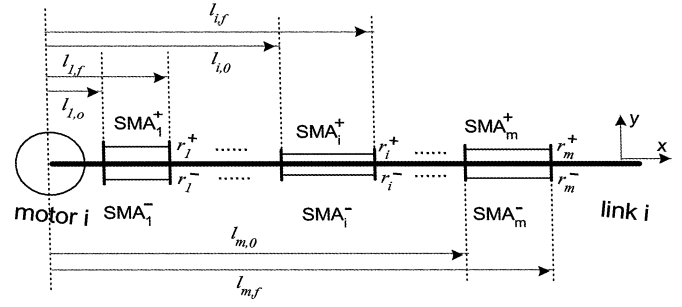


Fig. 1. m pairs of SMA actuators attached to the i th flexible link to suppress vibrations.

Based on [21]–[23], and for a uniform circular cross-sectional area, the force p_i induced in each SMA wire is given by

$$p_i = \frac{\pi d^2}{4} [E\varepsilon_i - \Phi\zeta_i(T_i, p_i) + \Upsilon(T_i - T_0)] \quad (1)$$

for $i = 1^+, 1^-, 2^+, 2^-, \dots, m^+, m^-$, where d is the diameter of the SMA wire, E is the average Young's modulus between the fully martensite and fully austenite phases, $\Phi = E\varepsilon_L > 0$ is the phase transformation modulus, with ε_L denoting the maximum residual strain, Υ is the thermoelastic modulus, ζ_i is the martensite fraction, T_0 is the temperature value at which the thermal strain is zero, and T_i is the temperature variable.

The martensite fraction $\zeta_i(T_i, p_i)$ in each SMA actuator is described by

$$\zeta_i = \begin{cases} \zeta_{Mi}, & M \\ \frac{\zeta_{Mi}}{2} \left[\cos \left(a_A \left(T_i - A_s - \frac{4p_i}{C_A \pi d^2} \right) \right) + 1 \right], & M \rightarrow A \\ \frac{1 - \zeta_{Ai}}{2} \cos \left(a_M \left(T_i - M_f - \frac{4p_i}{C_M \pi d^2} \right) \right) + \frac{1 + \zeta_{Ai}}{2}, & A \rightarrow M \\ \zeta_{Ai}, & A \end{cases} \quad (2)$$

where M denotes the martensite phase, A denotes the austenite phase, M_s and M_f are the no-load martensite phase start and final temperatures, respectively, A_s and A_f are the no-load austenite phase start and final temperatures, respectively, C_A , C_M , $a_A = \pi / (A_f - A_s)$ and $a_M = \pi / (M_s - M_f)$ are positive constants representing the material properties, ζ_{Mi} and ζ_{Ai} are the martensite fractions at the beginning of the martensite-to-austenite transformation and austenite-to-martensite transformation, respectively.

Following [24], the conditions for the martensite-to-austenite phase transformation $M \rightarrow A$ are given by

$$\dot{T}_i - \frac{4\dot{p}_i}{C_A \pi d^2} > 0, \quad A_s + \frac{4p_i}{C_A \pi d^2} \leq T_i \leq A_f + \frac{4p_i}{C_A \pi d^2} \quad (3)$$

while that for the austenite-to-martensite phase transformation $A \rightarrow M$ are given by

$$\dot{T}_i - \frac{4\dot{p}_i}{C_M \pi d^2} < 0, \quad M_f + \frac{4p_i}{C_M \pi d^2} \leq T_i \leq M_s + \frac{4p_i}{C_M \pi d^2}. \quad (4)$$

To establish the relationship between $\partial\zeta_i/\partial p_i$ and $\partial\zeta_i/\partial T_i$, we compute the following from (2):

$$\frac{\partial\zeta_i}{\partial p_i} = \begin{cases} 0, & M \\ \frac{2a_A\zeta_{Mi}}{C_A\pi d^2} \sin\left[a_A\left(T_i - A_s - \frac{4p_i}{C_A\pi d^2}\right)\right], & M \rightarrow A \\ \frac{2a_M(1-\zeta_{Ai})}{C_M\pi d^2} \sin\left[a_M\left(T_i - M_f - \frac{4p_i}{C_M\pi d^2}\right)\right], & A \rightarrow M \\ 0, & A \end{cases} \quad (5)$$

$$\frac{\partial\zeta_i}{\partial T_i} = \begin{cases} 0, & M \\ \frac{-a_A\zeta_{Mi}}{2} \sin\left[a_A\left(T_i - A_s - \frac{4p_i}{C_A\pi d^2}\right)\right], & M \rightarrow A \\ \frac{-a_M(1-\zeta_{Ai})}{2} \sin\left[a_M\left(T_i - M_f - \frac{4p_i}{C_M\pi d^2}\right)\right], & A \rightarrow M \\ 0, & A \end{cases} \quad (6)$$

from which it can be seen that

$$\frac{\partial\zeta_i}{\partial p_i} = -\frac{4}{C_{AM}\pi d^2} \frac{\partial\zeta_i}{\partial T_i} \quad (7)$$

where

$$C_{AM} := \begin{cases} C_A, & \text{for } A \rightarrow M \\ C_M, & \text{for } M \rightarrow A \end{cases} \quad (8)$$

Denote $\bar{T}_i := T_i - T_\infty$, where T_∞ is the ambient temperature. The temperature of the SMA actuators are governed by the heat transfer model [24] as follows:

$$\begin{aligned} \dot{\bar{T}}_i &= -\gamma\bar{T}_i + \lambda u_i - \frac{\Delta H}{c} \dot{\zeta}_i \\ &= \frac{1}{1 + \frac{\Delta H}{c} \frac{\partial\zeta_i}{\partial T_i}} \left[-\gamma\bar{T}_i + \lambda u_i - \frac{\Delta H}{c} \frac{\partial\zeta_i}{\partial p_i} \dot{p}_i \right] \end{aligned} \quad (9)$$

where u_i denotes the square of the current input, c the specific heat capacity, ΔH the latent heat associated with the phase transformation, and the coefficients γ and λ are given by

$$\gamma = \frac{4h_f}{\rho dc}, \quad \lambda = \frac{16\nu}{\rho\pi^2 d^4 c} \quad (10)$$

where h_f is the convection heat transfer coefficient, ρ is the density, and ν is the resistivity.

Remark 1: The slow response of the SMAs is a major limitation in practice. From the heat transfer equation (9), and the heat transfer coefficient γ in (10), we see that by reducing the actuator size, we can improve the heat transfer and accelerate the rate of response. However, from (1), it is clear that the force production decreases with size, thus diminishing the advantage of the SMAs in delivering large forces. For a successful implementation of the SMAs, engineers need to balance the force requirements of the application in concern with the rate of cooling that can be achieved in the operating environment.

To obtain the strain induced in the i th SMA wire ε_i , we consider the link deformation along the interval $x \in [l_{i,0}, l_{i,f}]$, where x is the longitudinal coordinate along the link, and $l_{i,0}, l_{i,f}$ denote the longitudinal positions of the points of attachment of the SMA wire. Assuming that the transverse and shear strains are negligible compared with the longitudinal strain, we first obtain the average strain ε_{ave} induced in the link along the interval

$x \in [l_{i,0}, l_{i,f}]$ as follows:

$$\varepsilon_{\text{ave}} = \frac{1}{l_{i,f} - l_{i,0}} \int_{l_{i,0}}^{l_{i,f}} -sy'' dx \quad (11)$$

where y is the vertical displacement, s denotes the transverse distance from the neutral plane to the surface of the link, and the operators $(\cdot)''$ and $(\cdot)'$ are defined by $\partial^2(\cdot)/\partial x^2$ and $\partial(\cdot)/\partial x$, respectively.

We approximate ε_i by $\varepsilon_i = \varepsilon_{\text{ave}}|_{s=r_i}$, where r_i denotes the moment arm. Based on the AMM with a finite-series truncated model comprising N dominant modes, the vertical displacement from the undeformed beam is given by

$$y(x, t) = \sum_{j=1}^N \psi_j(x) q_j(t) \quad (12)$$

where $\psi_j(x) \in R$ is the shape function for the j th mode, and $q_j(t)$, $j = 1, \dots, N$ are generalized coordinates to be explained in greater detail in Section II-B. Thus, we obtain an estimate of the strain induced in the SMA wire as

$$\varepsilon_i = -\frac{r_i}{l_{i,f} - l_{i,0}} \sum_{j=1}^{n_f} [\psi'_j(l_{i,f}) - \psi'_j(l_{i,0})] q_j(t). \quad (13)$$

From (1), it can be seen that p_i is an implicit function, and the appearance of p_i on the right-hand side (RHS) is nonaffine. Since it is difficult to express p_i explicitly in T_i , it poses a problem if one attempts to control p_i via the virtual control T_i , which is, in turn, controlled directly by u_i . By taking the time derivative of p_i , we obtain a differential equation in which u_i appears and can be used to control p_i directly. From (1) and (9), the time derivative of p_i can be obtained as

$$\dot{p}_i = \frac{\pi d^2}{4} \left[E\dot{\varepsilon}_i - \Phi \frac{\partial\zeta_i}{\partial p_i} \dot{p}_i + \left(\Upsilon - \Phi \frac{\partial\zeta_i}{\partial T_i} \right) \dot{\bar{T}}_i \right]. \quad (14)$$

Substituting (7) and (9) into (14), the derivative of p_i can be rewritten in the following compact form, which is affine in u_i :

$$\dot{p}_i = k(f_i(T_i, p_i, \dot{q}_i) + g_i(T_i, p_i)u_i) \quad (15)$$

$$\begin{aligned} f_i(T_i, p_i, \dot{q}_i) &= \frac{\pi d^2}{4k(1 + h_i(T_i, p_i))} \\ &\times \left[-\frac{Er_i(1 + \frac{\Delta H}{c} \frac{\partial\zeta_i}{\partial T_i})}{l_{i,f} - l_{i,0}} \sum_{j=1}^{n_f} [\psi'_j(l_{i,f}) - \psi'_j(l_{i,0})] \right. \\ &\left. \times \dot{q}_j(t) - \gamma \left(\Upsilon - \Phi \frac{\partial\zeta_i}{\partial T_i} \right) \bar{T}_i \right] \end{aligned} \quad (16)$$

where $k > 0$ is a scaling factor, $f(T_i, p_i, \dot{q}_i)$ is defined in (16), and $g_i(T_i, p_i)$ is given by (17)

$$g_i(T_i, p_i) = \frac{\pi d^2}{4k(1 + h_i(T_i, p_i))} \lambda \left(\Upsilon - \Phi \frac{\partial\zeta_i}{\partial T_i} \right) \quad (17)$$

with

$$h_i(T_i, p_i) = \left[\left(1 - \frac{\Upsilon}{C_A} \right) \frac{\Delta H}{c} - \frac{\Phi}{C_A} \right] \frac{\partial\zeta_i}{\partial T_i}. \quad (18)$$

Since E , Υ , and Ψ are large constants, the scaling factor k is large, and (15) as

$$\epsilon \dot{p}_i = \tilde{k}(f_i(T_i, p_i, \dot{q}) + g_i(T_i, p_i)u_i) \quad (19)$$

where $\tilde{k} = \epsilon k$ is non-negligible for some $0 < \epsilon \ll 1$. From (16), it is important to realize that since both f_i and g_i contain the term $h_i(T_i, p_i)$ in the denominator, singularities may occur. We address this issue with Property 1.

Property 1: The functions $f_i(T_i, p_i, \dot{q}) : R \times R \times R^{n_f} \mapsto R$ and $g_i(T_i, p_i) : R \times R \mapsto R$ do not contain any singularities provided that the system parameters satisfy the condition

$$a_{\max} \left[\left(1 - \frac{\Upsilon}{C_{\max}}\right) \frac{\Delta H}{c} - \frac{\Phi}{C_{\max}} \right] < 2 \quad (20)$$

where $a_{\max} := \max\{a_A, a_M\}$ and $C_{\max} := \max\{C_A, C_M\}$.

Proof: We need to prove that the function $h_i(T_i, p_i)$ is bounded away from $-1 \forall T, p \in R$, so that the denominators of $f_i(\cdot)$ and $g_i(\cdot)$ do not have any zero crossings. From (6), it is clear that the phase regions M and A trivially satisfy $h_i \neq -1$. We will now consider $M \rightarrow A$ and $A \rightarrow M$.

For $M \rightarrow A$, we know, from (3), that $0 \leq a_A(T_i - A_s - (4p_i/C_A \pi d^2)) \leq \pi$, and thus, $0 \leq \sin[a_A(T_i - A_s - (4p_i/C_A \pi d^2))] \leq 1$. It follows from (6) that

$$-\frac{a_A \zeta_{M_i}}{2} \leq \frac{\partial \zeta_i}{\partial T_i} \leq 0. \quad (21)$$

The condition for $h_i \neq -1$ is equivalent to $h_i > -1$ or $h_i < -1$. However, from (18) and (21), it is clear that $h_i < -1$ is not admissible when $\partial \zeta_i / \partial T_i = 0$, which implies $h_i = 0$. Therefore, we only consider the case $h_i > -1$, which can be rewritten as

$$\begin{aligned} -\frac{a_A \zeta_{M_i}}{2} \left[\left(1 - \frac{\Upsilon}{C_A}\right) \frac{\Delta H}{c} - \frac{\Phi}{C_A} \right] &> -1 \\ \Rightarrow a_A \left[\left(1 - \frac{\Upsilon}{C_A}\right) \frac{\Delta H}{c} - \frac{\Phi}{C_A} \right] &< 2 \end{aligned} \quad (22)$$

since $0 \leq \zeta_{M_i} \leq 1$. This condition on the parameters ensures that $h_i(T_i, p_i)|_{M \rightarrow A}$ is bounded away from -1 .

A similar analysis applies for the case of $A \rightarrow M$, where we can obtain

$$a_M \left[\left(1 - \frac{\Upsilon}{C_M}\right) \frac{\Delta H}{c} - \frac{\Phi}{C_M} \right] < 2 \quad (23)$$

which ensures that $h_i(T_i, p_i)|_{A \rightarrow M}$ is bounded away from -1 .

Combining (22) and (23), we obtain (20). Since $h_i(T_i, p_i) > -1 \forall T_i, p_i \in R$, hence, the denominator term $k(1 - h_i(T_i, p_i)) > 0$ in (16) and (17). Then, it can be concluded that $f_i(T_i, p_i, \dot{q})$ and $g_i(T_i, p_i)$ are free of singular points $\forall T_i, p_i \in R, \dot{q} \in R^{n_f}$ given that the condition (20) holds. ■

To analyze the controllability of the SMA actuator dynamics, we establish the following property.

Property 2: For any $T_i, p_i \in R$, there exists a constant \underline{g}_i such that the function $g_i(T_i, p_i)$ in (17) satisfies $g_i(T_i, p_i) > \underline{g}_i > 0$, if condition (20) holds. Hence, $g_i(T_i, p_i)$ is always positive and does not have any zero crossings, implying that the SMA dynamics (15)–(18) always satisfy the controllability condition.

Proof: We need to show that the terms $[\Upsilon - (\Phi(\partial \zeta_i / \partial T_i))]$ and $[\pi d^2 / [4k(1 + h_i(T_i, p_i))]]$ from (17) are both strictly positive. Since Υ and Φ are positive constants, and $\partial \zeta_i / \partial T_i \leq 0$, it is clear that $[\Upsilon - (\Phi(\partial \zeta_i / \partial T_i))] > 0$.

From the proof of Property 1, we know that $h_i(T_i, p_i) > -1$ if condition (20) holds, for any $T_i, p_i \in R$. From (18), (21), and the fact that $-[a_M(1 - \zeta_{A_i})] / 2 \leq \partial \zeta_i / \partial T_i \leq 0$, it can be deduced that h_i is upper bounded as follows:

$$h_i(T_i, p_i) \leq \frac{1}{2} \left[\left(1 - \frac{\Upsilon}{C_A}\right) \frac{\Delta H}{c} - \frac{\Phi}{C_A} \right] a_{\max} =: \bar{h}_i \quad (24)$$

where $\bar{h}_i > 0$ is a constant, which leads to

$$\frac{\pi d^2}{4k(1 + h_i(T_i, p_i))} \geq \frac{\pi d^2}{4k(1 + \bar{h}_i)} > 0. \quad (25)$$

Therefore, since $\pi d^2 / [4k(1 + h_i(T_i, p_i))] > 0$ and $[\Upsilon - (\Phi(\partial \zeta_i / \partial T_i))] > 0$, it can be concluded from (17) that $g_i(T_i, p_i) > \underline{g}_i > 0$ holds. ■

B. Flexible Robot Dynamics

Consider a multi-link flexible robot with rotational joints, operating on the horizontal plane. The SMA actuators are attached to each flexible link for the vibration suppression. One end of each link is rigidly attached to the rotor of a motor, and the tip payload is considered as a point mass. In order to find the dominant physical properties of the system and to simplify the model, it is assumed that each link has a sufficiently small thickness, such that the deflection is solely a function of x and independent of the thickness.

The control objective is to track a desired trajectory $\theta_d(t)$ while suppressing the vibrations of the flexible links. At the same time, all the closed loop signals are to be kept bounded.

Using the AMM, the dynamical equations for the motion and vibration of the flexible robot can be obtained as

$$M(\theta, q) \begin{bmatrix} \ddot{\theta} \\ \ddot{q} \end{bmatrix} = C(\theta, \dot{\theta}, q, \dot{q}) \begin{bmatrix} \dot{\theta} \\ \dot{q} \end{bmatrix} - \begin{bmatrix} 0 \\ K_q q \end{bmatrix} + \begin{bmatrix} \tau \\ BP \end{bmatrix} \quad (26)$$

where $\theta \in R^{n_r}$ denotes the rigid variables and $q \in R^{n_f}$ denotes the flexible variables, $\tau \in R^{n_r}$ is the vector of torques applied at the joints, $P = \{p_i^+, p_i^-\} \in R^{2m}$ for $i = 1, \dots, m$ is the vector of forces induced in m pairs of the SMA wires, with p_i^\pm representing the force in each SMA wire as in (1), $B \in R^{n_f \times 2m}$ is the input gain matrix for the flexible subsystem, $K_q \in R^{n \times n}$ is the stiffness matrix of the flexible robot, and

$$M(\theta, q) := \begin{bmatrix} M_{\theta\theta} & M_{\theta q} \\ M_{q\theta} & M_{qq} \end{bmatrix} \in R^{n \times n}$$

is the symmetric positive definite inertia matrix and

$$C(\theta, \dot{\theta}, q, \dot{q}) := \begin{bmatrix} C_{\theta\theta} & C_{\theta q} \\ C_{q\theta} & C_{qq} \end{bmatrix} \in R^{n \times n}$$

represents the matrix coefficients that give the Coriolis and centrifugal forces.

Proposition 1: The input coefficient matrix for a flexible sub-system B is given by

$$B = \begin{bmatrix} r_1^+ \varphi_{1,1} & -r_1^- \varphi_{1,1} & \cdots & r_m^+ \varphi_{1,m} & -r_m^- \varphi_{1,m} \\ \cdots & \cdots & \cdots & \cdots & \cdots \\ r_1^+ \varphi_{n_f,1} & -r_1^- \varphi_{n_f,1} & \cdots & r_m^+ \varphi_{n_f,m} & -r_m^- \varphi_{n_f,m} \end{bmatrix} \quad (27)$$

$$\varphi_{j,i} = \int_{l_{i,0}}^{l_{i,f}} \psi_j''(x) dx = \psi_j'(l_{i,f}) - \psi_j'(l_{i,0}) \quad (28)$$

where r_i for $i = 1, \dots, m$ are the moment arms of the SMA wires, $\psi_j(x) \in R$ for $j = 1, \dots, n_f$ are the modal shape functions, with x as the longitudinal coordinate along the link.

Proof: The proof of Proposition 1 is straightforward using the method of virtual work, and hence, is omitted. ■

Property 3: Because $\dot{M} - 2C$ is skew-symmetric as in the rigid robot case, we know that $\dot{M}_{\theta\theta} - 2C_{\theta\theta}$ is correspondingly skew-symmetric.

For the ease of notation, we denote M^{-1} by

$$H = \begin{bmatrix} H_{\theta\theta} & H_{\theta q} \\ H_{q\theta} & H_{qq} \end{bmatrix}.$$

We can rewrite (26) into the standard singular perturbation form

$$\begin{aligned} \ddot{\theta} &= -H_{\theta\theta}(C_{\theta\theta}\dot{\theta} + C_{\theta q}\epsilon^2\dot{\xi}) - H_{\theta q}(C_{q\theta}\dot{\theta} + C_{qq}\epsilon^2\dot{\xi}) \\ &\quad - H_{\theta q}\tilde{K}\xi + H_{\theta\theta}\tau + H_{\theta q}BP \\ \epsilon^2\ddot{\xi} &= -H_{q\theta}(C_{\theta\theta}\dot{\theta} + C_{\theta q}\epsilon^2\dot{\xi}) - H_{qq}(C_{q\theta}\dot{\theta} + C_{qq}\epsilon^2\dot{\xi}) \\ &\quad - H_{qq}\tilde{K}\xi + H_{q\theta}\tau + H_{qq}BP \end{aligned} \quad (29)$$

where $\xi := (1/\epsilon^2)q$ and $\tilde{K} := \epsilon^2 K_q$ are new variables, with ϵ being a small positive constant.

1) *Slow Subsystem:* To identify the slow subsystem, we set $\epsilon = 0$ and solve (29) for ξ to obtain

$$\bar{\xi} = \tilde{K}^{-1}[\bar{H}_{qq}^{-1}\bar{H}_{q\theta}(-\bar{C}_{\theta\theta}\dot{\bar{\theta}} + \bar{\tau}) - \bar{C}_{q\theta}\dot{\bar{\theta}} + B\bar{P}] \quad (30)$$

where a bar indicates that the said variable is considered with $\epsilon = 0$. Substituting (30) into (29) with $\epsilon = 0$ leads to

$$\ddot{\bar{\theta}} = (\bar{H}_{\theta\theta} - \bar{H}_{\theta q}\bar{H}_{qq}^{-1}\bar{H}_{q\theta})(-\bar{C}_{\theta\theta}\dot{\bar{\theta}} + \bar{\tau}). \quad (31)$$

It can be shown that the above equation is equivalent to

$$\bar{M}_{\theta\theta}\ddot{\bar{\theta}} + \bar{C}_{\theta\theta}\dot{\bar{\theta}} = \bar{\tau} \quad (32)$$

which corresponds to the rigid body robot dynamic model.

2) *Fast Subsystem:* To identify the fast subsystem, define a fast time scale $\tau_t = t/\epsilon$, boundary layer correction variables $z_1 = \xi - \bar{\xi}$, $z_2 = \epsilon\dot{\xi}$, and $z_3 = \bar{H}_{qq}BP$. From (29) and the fact that $d\bar{\xi}/d\tau_t = \epsilon\dot{\bar{\xi}} = 0$, the fast subsystem is given by

$$\begin{aligned} \frac{dz_1}{d\tau_t} &= z_2 \\ \frac{dz_2}{d\tau_t} &= -H_{q\theta}(C_{\theta\theta}\dot{\theta} + C_{\theta q}\epsilon z_2 - H_{qq}(C_{q\theta}\dot{\theta} + C_{qq}\epsilon z_2) \\ &\quad - H_{qq}\tilde{K}(z_1 + \bar{\xi}) + H_{q\theta}\tau + H_{qq}BP \\ \frac{dP}{d\tau_t} &= \tilde{k}[f(T, P, \epsilon z_2) + G(T, P)u] \end{aligned} \quad (33)$$

where $f = \{f_i^+, f_i^-\} \in R^{2m}$ for $i = 1, \dots, m$, the vector of the temperature signals is given by $T = \{T_i^+, T_i^-\} \in R^{2m}$ for $i = 1, \dots, m$, the vector of the control input is denoted by $u = \{u_i^+, u_i^-\} \in R^{2m}$ for $i = 1, \dots, m$, and $G = \text{diag}\{g_i^+, g_i^-\} \in R^{2m \times 2m}$ for $i = 1, \dots, m$.

From (1), it can be seen that T is a function of P and q . Since $P : z_3 \mapsto P(z_3)$ and $q : z_1 \mapsto q(z_1)$, hence, we know that $T : (z_1, z_3) \mapsto T(z_1, z_3)$. Setting $\epsilon = 0$ and substituting $\bar{\xi}$ from (30) into (33), we get

$$\begin{aligned} \frac{dz_1}{d\tau_t} &= z_2 \\ \frac{dz_2}{d\tau_t} &= -\bar{H}_{qq}\tilde{K}z_1 + z_3 \\ \frac{dz_3}{d\tau_t} &= \tilde{k}\bar{H}_{qq}B[\bar{f}(z_1, z_3) + G(z_1, z_3)u] \end{aligned} \quad (34)$$

where $\bar{f} := f|_{\epsilon=0}$, which yields a nonlinear system in a strict feedback form parameterized in the slow variable $\bar{\theta}$.

III. COMPOSITE CONTROL FOR FAST AND SLOW SUBSYSTEMS

A. Control for Slow Subsystem

Given that the desired trajectory $\theta_d(t) \in R^{n_r}$ is twice differentiable for the slow dynamics, the slow subsystem is given by

$$\bar{M}_{\theta\theta}\dot{e}_r = -\bar{C}_{\theta\theta}e_r - \bar{\tau} + \bar{M}_{\theta\theta}\ddot{\theta}_v + \bar{C}_{\theta\theta}\dot{\theta}_v \quad (35)$$

where the tracking error is $e = \theta_d - \bar{\theta}$, $\dot{\theta}_v = \dot{\theta}_d + \Lambda e$, and $e_r = \dot{\theta}_v - \dot{\bar{\theta}} = \dot{e} + \Lambda e$, with Λ being a symmetric positive definite matrix. Choosing the control torque as

$$\bar{\tau} = \bar{M}_{\theta\theta}\ddot{\theta}_v + \bar{C}_{\theta\theta}\dot{\theta}_v + K_p e_r \quad (36)$$

where $K_p > 0$, the closed loop error dynamics are reduced to

$$\bar{M}_{\theta\theta}\dot{e}_r + \bar{C}_{\theta\theta}e_r + K_p e_r = 0. \quad (37)$$

Theorem 1: The slow subsystem given in (35) under the control law (36) has an asymptotically stable solution $(e, \dot{e}) = 0$, in the sense that as $t \rightarrow \infty$, we have $e(t) \rightarrow 0$ and $\dot{e}(t) \rightarrow 0$.

Proof: Consider the Lyapunov function candidate $V = (1/2)e_r^T \bar{M}_{\theta\theta} e_r$, for which the time derivative along (35) and (36), with the help of Property 3, can be obtained as $\dot{V} = -e_r^T K_p e_r \leq 0$, which leads to

$$\lambda_{\min}(K_p) \int_0^t e_r^T e_r d\tau \leq \int_0^t e_r^T K_p e_r d\tau \leq V(0) \quad (38)$$

where $\lambda_{\min}(\cdot)$ denotes the minimum eigenvalue of (\cdot) .

Since $V(0)$ and $\lambda_{\min}(K_p)$ are positive constants, it follows that $e_r \in L_{n_r}^2$. This implies that $e \in L_{n_r}^2$; e is continuous and $e \rightarrow 0$ as $t \rightarrow \infty$; and $\dot{e} \in L_{n_r}^2$.

Furthermore, since $\dot{V} \leq 0$, we know that $0 \leq V(t) \leq V(0)$, $\forall t \geq 0$. Thus, it follows from $V(t) \in L^\infty$ that $\int_0^t d\tau \in L^\infty$.

Noting that $e_r \in L_{n_r}^2$ and $\theta_d, \dot{\theta}_d, \ddot{\theta}_d \in L_{n_r}^\infty$, it can be concluded from (37) that $\dot{e} \in L_{n_r}^\infty$, which implies that e_r is uniformly continuous. From the fact that e_r is uniformly continuous and $e_r \in L_{n_r}^2$, it follows that $e_r \rightarrow 0$ as $t \rightarrow \infty$, and thus, $\dot{e} \rightarrow 0$ as $t \rightarrow \infty$. ■

B. Control for Fast Subsystem

It can be seen that the fast subsystem, as described by (34), is in a strict feedback form, for which we can employ backstepping to derive a stable controller u as follows.

Step 1: Consider the first equation of (34). Define $\eta_1 = z_1$ and $\eta_2 = z_2 - \alpha_1$, where α_1 is a smooth virtual control. Choose Lyapunov function $V_1 = (1/2)\eta_1^T \eta_1$ and virtual control

$$\alpha_1 = -K_1 \eta_1. \quad (39)$$

Taking the time derivative along (34) leads to

$$\frac{dV_1}{d\tau_t} = -\eta_1^T K_1 \eta_1 + \eta_1^T \eta_2 \quad (40)$$

where the term $\eta_1^T \eta_2$ will be canceled in the following step.

Step 2: Consider the second equation of (34). Define $\eta_3 = z_3 - \alpha_2$, where α_2 is a smooth virtual control. Choose Lyapunov function $V_2 = V_1 + (1/2)\eta_2^T \eta_2$ and virtual control

$$\alpha_2 = (\bar{H}_{qq} \bar{K} - I_{n_f}) \eta_1 - K_2 \eta_2 + \frac{d\alpha_1}{d\tau_t}. \quad (41)$$

Taking the time derivative along (34) leads to

$$\frac{dV_2}{d\tau_t} = -\sum_{i=1}^2 \eta_i^T K_i \eta_i + \eta_2^T \eta_3 \quad (42)$$

where the term $\eta_2^T \eta_3$ will be canceled in the following step.

Step 3: In the final step, choose Lyapunov function $V_3 = V_2 + (1/2)\eta_3^T \bar{H}_{qq}^{-1} \eta_3$. If we suppose that the actual control u can take both positive and negative values, then, it can be designed as

$$u = G^{-1} \left[-\bar{f} - \frac{1}{k} U B^+ \left(\eta_2 + K_3 \eta_3 - \bar{H}_{qq}^{-1} \frac{d\alpha_2}{d\tau_t} \right) \right] \quad (43)$$

where $\bar{f}(T, P) := f(T, P, \epsilon z_2)|_{\epsilon=0}$; and the right inverse $B^+ \in R^{2m \times n_f}$ and the permutation matrix $U \in R^{2m \times 2m}$ satisfy $BUB^+ = I$. Note that $G^{-1}(T, p)$ is well defined since $G(T, p)$ is a diagonal matrix with strictly positive elements, as shown in Property 2. Taking the time derivative along (34) would lead to $dV_3/d\tau_t = -\sum_{i=1}^3 \eta_i^T K_i \eta_i$, from which we can conclude the asymptotic stability of $\eta = 0$.

However, the input u cannot assume negative values since it is defined as the square of current. As a result, (43) is not a feasible design. To circumvent this problem, we exploit the property of the control coefficient matrix B in (27) stemming from the antagonist pair configuration of the SMA actuators.

First, we note that (27) can be rewritten as $B = \bar{B}\Gamma$, where $\Gamma := \text{blockdiag}\{[1 - \beta_j]\}$, $\beta_j = r_j^-/r_j^+ > 0$, for $j = 1, \dots, m$, and

$$\bar{B} := \begin{bmatrix} r_1^+ \varphi_{1,1} & \cdots & r_j^+ \varphi_{1,j} & \cdots & r_m^+ \varphi_{1,m} \\ \vdots & \ddots & \vdots & \ddots & \vdots \\ r_1^+ \varphi_{n_f,1} & \cdots & r_j^+ \varphi_{n_f,j} & \cdots & r_m^+ \varphi_{n_f,m} \end{bmatrix}. \quad (44)$$

Hence, the following relationship holds:

$$B [\bar{f}(T, P) + G(T, P)u] = \bar{B} [\bar{F}(T, P) + v] \quad (45)$$

where $\bar{F} := \Gamma \bar{f} \in R^m$, and $v = \Gamma G u \in R^m$ is a new control, which can be shown to be in the form

$$v_j = g_j^+ u_j^+ - \beta_j g_j^- u_j^-, \quad j = 1, \dots, m. \quad (46)$$

The new control is chosen as

$$v = -\bar{F}(T, P) - \frac{1}{k} \bar{U} \bar{B}^+ \left(\eta_2 + K_3 \eta_3 - \bar{H}_{qq}^{-1} \frac{d\alpha_2}{d\tau_t} \right) \quad (47)$$

such that

$$\frac{dV_3}{d\tau_t} = -\sum_{i=1}^3 \eta_i^T K_i \eta_i \quad (48)$$

where the right inverse $\bar{B}^+ \in R^{2m \times n_f}$ and the permutation matrix $\bar{U} \in R^{2m \times 2m}$ satisfy $\bar{B} \bar{U} \bar{B}^+ = I$. Given that B is full rank, the right inverse \bar{B}^+ always exists. Note that B can be ensured to be full rank by an appropriate design of the actuator configuration. In particular, the values of r_i^+ , $l_{i,0}$, and $l_{i,f}$, for $i = 1, \dots, m$, are to be chosen such that $[r_i^+ \varphi_{1,i}, \dots, r_i^+ \varphi_{n_f,i}]^T$, $i = 1, 3, \dots, 2m - 1$, i.e., the odd columns of B , are linearly independent vectors, since the even-column vectors are simply scalings of the preceding odd-column counterparts.

Each signal in (47) is, then, apportioned between the two actuators in each antagonist pair using the following algorithm:

$$u_j^+ = \frac{1}{g_j^+} \sigma_{\{v_j > 0\}} v_j, \quad u_j^- = -\frac{1}{\beta_j g_j^-} \sigma_{\{v_j < 0\}} v_j \quad (49)$$

for $j = 1, \dots, m$, where $\sigma_{\{\bullet\}} = 1$ if \bullet is true, and 0 otherwise. It can be checked that (49) satisfies (46), and that u_j^+ and u_j^- are always non-negative.

Theorem 2: The origin of the fast subsystem (34) under condition (20) and the backstepping control law (49) is uniformly exponentially stable in $(t, \theta) \in [0, t_1] \times \Theta$ for $\Theta \subset R^{n_f}$.

Proof: From (48), we have that $dV_3/d\tau_t \leq -\mu V_3$, where

$$\mu := 2 \left(\lambda_{\min}(K_1), \lambda_{\min}(K_2), \frac{\lambda_{\min}(K_3)}{\lambda_{\max}(\bar{H}_{qq})} \right)$$

with $\lambda_{\min}(\cdot)$ and $\lambda_{\max}(\cdot)$ denoting the minimum and maximum eigenvalues of (\cdot) , respectively. As a result, we obtain that $V_3(\tau_t) \leq V_3(0)e^{-\mu\tau_t}$, from which it can be shown that

$$\|\eta(\tau_t)\| \leq \varrho_1 \|\eta(0)\| e^{-\varrho_2 \tau_t} \quad (50)$$

where

$$\varrho_1 = \sqrt{\frac{\max(1/2, \lambda_{\max}(\bar{H}_{qq}^{-1}))}{\min(1/2, \lambda_{\min}(\bar{H}_{qq}^{-1}))}}$$

and $\varrho_2 = \mu/2$. Thus, the exponential stability of the solution $\eta = 0$ is obtained. ■

Corollary 1: The temperature signal $T(\tau_t)$ in the closed loop fast subsystem comprising (34) and (49) is bounded for all $\tau_t > 0$.

Proof: From (50), it is clear that $\|\eta_j(\tau_t)\| \leq \varrho_1 \|\eta_j(0)\|$ for $j = 1, 2, 3$. Hence, we know that $\|z_1(\tau_t)\| \leq \varrho_1 \|z_1(0)\|$, which implies that the virtual control $\alpha_1(\tau_t)$ given in (39) is bounded. Since $z_2 = \eta_2 + \alpha_1$, it follows that $z_2(\tau_t)$ is bounded. This implies that the virtual control $\alpha_2(\tau_t)$ given in (41) is also bounded. Since $z_3 = \eta_3 + \alpha_2$, we know that $z_3(\tau_t)$ is bounded. From the

definition $z_3(\tau_t) = \bar{H}_{qq}BP(\tau_t)$, it is easy to see that $P(\tau_t)$ is bounded.

From (1), (13), and the fact that $q = \epsilon^2(z_1 + \bar{\xi})$, we obtain that

$$p_i = \frac{\pi d^2}{4} [\epsilon^2 E \Psi_i^T(z_1 + \bar{\xi}) - \Phi \zeta_i(T_i, p_i) + \Upsilon(T_i - T_0)]$$

for $i = 1^+, 1^-, \dots, m^+, m^-$, where $\Psi_i := -r_i / (l_{i,f} - l_{i,0}) [\psi'_1(l_{i,f}) - \psi'_1(l_{i,0}), \dots, \psi'_{n_f}(l_{i,f}) - \psi'_{n_f}(l_{i,0})]^T$.

Since $0 \leq \zeta_i(T_i, p_i) \leq 1$ and $p_i(\tau_t)$, $\bar{\xi}(\tau_t)$, and $z_1(\tau_t)$ are bounded, we can conclude the boundedness of $T_i(\tau_t)$ for all $\tau_t > 0$. ■

Given that the slow and fast subsystems are separately stabilized, we invoke Tikhonov's theorem to conclude the boundedness of the errors that arise in reality from the nonzero constant ϵ .

Theorem 3 (Tikhonov's theorem): If the slow subsystem has a unique solution defined on an interval $t \in [0, t_1]$, and if the fast subsystem is uniformly exponentially stable in (t, θ) , then there exists ϵ^* such that for all $\epsilon < \epsilon^*$, we have

$$\begin{aligned} \xi(t) &= \bar{\xi}(t) + z_1(\tau_t) + O(\epsilon) \\ \theta(t) &= \bar{\theta}(t) + O(\epsilon). \end{aligned} \quad (51)$$

Proof: The detailed proof can be found in [25]. ■

Therefore, from Corollary 1 and Theorem 3, we can conclude that the joint angle θ of the flexible robot stays within a small neighborhood $O(\epsilon)$ of the desired trajectory θ_d , and the vibration modes stay within a small neighborhood $O(\epsilon)$ of the origin, while all the other closed loop signals remain bounded.

IV. SIMULATION STUDY

To demonstrate the effectiveness of the proposed control scheme for the SMA-based flexible robot, numerical simulations are performed for a single-link robot operating on the horizontal plane. The SMA-based flexible robot is simulated using a two-mode dynamic model (the parameters are indicated in Table I), with the SMA parameter values based on [24], [26]. We consider two pairs of SMA actuators with the following parameters: $r_1^+ = r_1^- = r_2^+ = r_2^- = 2.0$ cm, $l_{1,0} = 0.0$ m, $l_{1,f} = 0.5$ m, $l_{2,0} = 0.5$ m, and $l_{2,f} = 1.0$ m. The control parameters are selected as $K_p = 10.0$, $K_1 = K_2 = K_3 = 0.2I$, $\epsilon = 0.127$.

To verify that condition (20) is satisfied such that Properties 1 and 2 hold, i.e., functions $f_i(\cdot)$ and $g_i(\cdot)$ in (16) and (17), respectively, are well defined, and the system is free of the control singularity, we substitute the parameter values from Table I into the left-hand side (LHS) of (20) as follows:

$$a_{\max} \left[\left(1 - \frac{\Upsilon}{C_{\max}} \right) \frac{\Delta H}{c} - \frac{\Phi}{C_{\max}} \right] = -11.9 < 2. \quad (52)$$

We investigate two types of desired trajectories, one of which terminates motion within a finite time, and the other is a periodic motion that extends to an infinite time. The first trajectory is given by a Hermite quintic polynomial in time t with a continuous bounded position, velocity, and bounded acceleration.

TABLE I
SYSTEM PARAMETERS

Description	Symbol [unit]	Value
Length of link	$L[m]$	1.0
Mass of link	$m[kg]$	0.1
Hub inertia	$I_h[kgm^2]$	3.0
Flexural rigidity of link	$EI[Nm^2]$	5.0
Heat convection coefficient	$h_f[Wm^{-2}K^{-1}]$	150.0
Density of NiTi	$\rho[gcm^{-3}]$	6.45
Specific heat of NiTi	$c[Jkg^{-1}K^{-1}]$	322.6
Electrical resistivity of NiTi	$\nu[\mu\Omega cm]$	80.0
Elastic modulus for austenite	$E_a[GPa]$	75.0
Elastic modulus for martensite	$E_m[GPa]$	28.0
Thermoelastic modulus	$\Upsilon[MPaK^{-1}]$	0.55
Load coefficient (austenite)	$C_A[MPaK^{-1}]$	10.3
Load coefficient (martensite)	$C_M[MPaK^{-1}]$	10.3
Austenite \rightarrow Martensite start temp	$A_s[^\circ C]$	68.0
Austenite \rightarrow Martensite end temp	$A_f[^\circ C]$	78.0
Martensite \rightarrow Austenite start temp	$M_s[^\circ C]$	52.0
Martensite \rightarrow Austenite end temp	$M_f[^\circ C]$	42.0
Ambient temperature	$T_\infty[^\circ C]$	20.0
Phase transformation modulus	$\Phi[GPa]$	1.12
Diameter of SMA wire	$d[mm]$	0.5
Latent heat of phase transformation	$\Delta H[Jg^{-1}]$	24.2

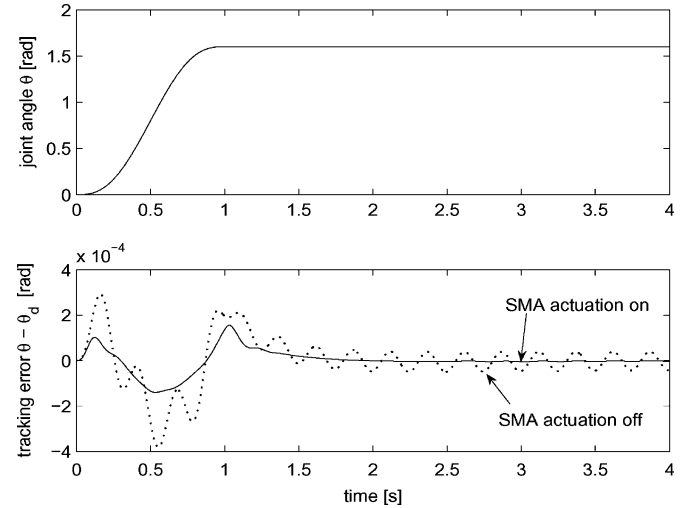


Fig. 2. Joint angle and tracking error.

The desired position trajectory can be written as

$$D1: \quad \theta_d(t) = \theta_0 + \left(\frac{6}{t_d^5} t^5 - \frac{15}{t_d^4} t^4 + \frac{10}{t_d^3} t^3 \right) (\theta_f - \theta_0) \quad (53)$$

where θ_0 is the desired initial position, θ_f is the desired final position, t_d is the time to reach θ_f , starting from θ_0 . In this paper, we set $\theta_0 = 0.0$ rad, $\theta_f = 1.6$ rad, and $t_d = 1.0$ s.

The second desired trajectory is described by a sinusoidal function

$$D2: \quad \theta_d(t) = (\theta_f - \theta_0) \sin \omega_d t \quad (54)$$

where we set $\theta_0 = 0.0$ rad, $\theta_f = 2.0$ rad, and $\omega_d = 1.26$ rad s^{-1} .

The simulation results in Figs. 2–4 pertain to the first case D1. From Fig. 2, it can be seen that the joint angle tracking error is very small, and that the SMA actuators are effective in

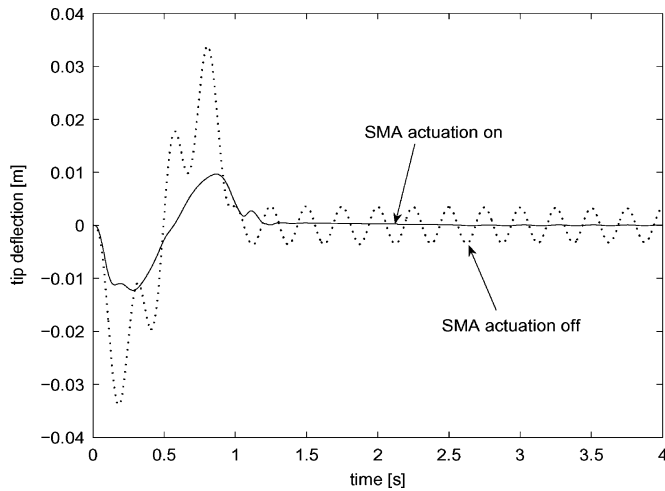


Fig. 3. Tip deflection of flexible link.

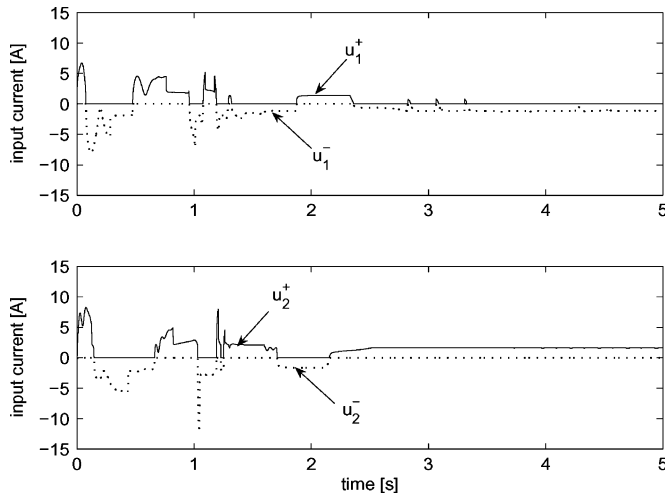


Fig. 4. Current inputs to the SMA actuators.

suppressing the residual vibrations. In the absence of the SMA-based vibration control, the residual tracking error is oscillatory and decays very slowly.

The tip deflection is shown in Fig. 3, where it is seen that the vibrations are effectively damped out by our SMA control scheme. In the case where SMA actuation is off, the flexible link experiences oscillatory tip deflection with a large amplitude of about 2.5 cm. The bounded control inputs are shown in Fig. 4.

For the second case D2, where the motion does not stop in a finite time, we can see from Fig. 5 that the tip deflection cannot be fully suppressed, unlike the case of D1. Nevertheless, the tracking error approaches zero and significant attenuation of the high-frequency vibrations is achieved as compared to the case where the SMA actuators are inactive. As in the case of D1, all the closed loop signals are bounded, but we omit the results for brevity.

Remark 2: The flexural rigidity was chosen to be rather low in order to induce larger amplitude vibrations to test the effectiveness of the proposed control. For the lightweight robots with long and slender links, it is reasonable for the vibrations to be dominated by the low-frequency modes.

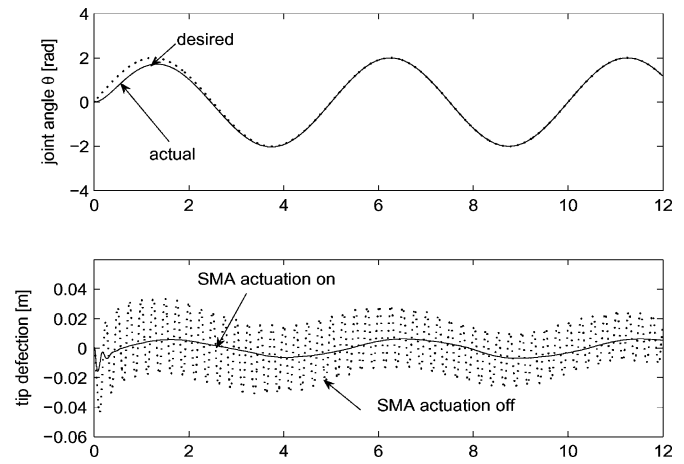


Fig. 5. Tracking performance and tip deflection for sinusoidal trajectory.

V. CONCLUSION

We have tackled the tracking control problem for the multi-link flexible robots requiring simultaneous suppression of vibrations. Singular perturbation theory has been used to model the full dynamics as two subsystems with time scale separation. Exploiting the stability properties of the two subsystems, Tikhonov's theorem has been invoked to show that the error between the state errors arising from the nonideal time scale separation ($\epsilon \neq 0$) is small. Simulation results have demonstrated that the proposed SMA control scheme leads to an improvement of the tracking performance and vibration suppression.

REFERENCES

- [1] R. H. Cannon, Jr. and E. Schmitz, "Initial experiments on the end-point control of a flexible robot," *Int. J. Robot. Res.*, vol. 3, no. 3, pp. 62–75, 1984.
- [2] A. Arakawa, T. Fukuda, and F. Hara, " H_∞ control of a flexible robotic arm (effect of parameter uncertainties on stability)," in *Proc. IEEE/RSJ Int. Workshop Intell. Robots Syst. (IROS)*, 1991, pp. 959–964.
- [3] B. Siciliano and W. J. Book, "A singular perturbation approach to control of lightweight flexible manipulator," *Int. J. Robot. Res.*, vol. 7, no. 4, pp. 79–89, 1998.
- [4] Z. H. Luo, "Direct strain feedback control of flexible robot arm: New theoretical and experimental results," *IEEE Trans. Autom. Control*, vol. 38, no. 11, pp. 1610–1622, Nov. 1993.
- [5] G. Zhu and S. Ge, "A quasitracking approach for finite-time control of a mass-beam system," *Automatica*, vol. 34, no. 7, pp. 881–888, 1998.
- [6] S. S. Ge, T. Lee, and G. Zhu, "Asymptotically stable end-point regulation of a flexible scara/cartesian robot," *IEEE/ASME Trans. Mechatronics*, vol. 3, no. 2, pp. 138–144, Jun. 1998.
- [7] S. S. Ge, "Adaptive controller design for flexible joint manipulator," *Automatica*, vol. 32, no. 6, pp. 273–248, 1996.
- [8] S. S. Ge, T. H. Lee, and Z. Wang, "Adaptive neural network control for smart materials robots using singular perturbation technique," *Asian J. Control*, vol. 3, no. 2, pp. 143–155, 2001.
- [9] S. S. Ge, T. Lee, and G. Zhu, "Energy-based robust controller design for multilink flexible robots," *Mechatronics*, vol. 6, no. 7, pp. 779–798, 1996.
- [10] S. S. Ge, T. H. Lee, and Z. Wang, "Model-free regulation of multilink smart materials robots," *IEEE/ASME Trans. Mechatronics*, vol. 6, no. 3, pp. 346–351, Sep. 2001.
- [11] K. Arai, S. Aramaki, and Y. Yanagisawa in *Proc. IEEE Int. Symp. Micro Mach. Human Sci.*, 1994, pp. 97–99.
- [12] R. B. Gorbet and D. Wang, "General stability criteria for a shape memory position control system," in *Proc. IEEE Int. Conf. Robot. Autom.*, vol. 3, 1995, pp. 2313–2319.
- [13] S. Majima, K. Kodama, and T. Hasegawa, "Modeling of shape memory alloy actuator and tracking control system with the model," *IEEE Trans. Control Syst. Technol.*, vol. 9, no. 1, pp. 54–59, Jan. 2001.

- [14] K. Arai, S. Aramaki, and Y. Yanagisawa, "Feedback linearization of SMA (shape memory alloy)," in *Proc. 34th SICE Annu. Conf.*, 1995, pp. 519–522.
- [15] D. Grant and V. Hayward, "Variable structure control of shape memory alloy actuators," *IEEE Control Syst. Mag.*, vol. 17, no. 3, pp. 80–88, Jun. 1997.
- [16] H. J. Lee and J. J. Lee, "Time delay control of a shape memory alloy actuator," *Smart Mater. Struct.*, vol. 13, pp. 227–239, 2004.
- [17] G. Song, V. Chaudhry, and C. Batur, "Precision tracking control of shape memory alloys actuators using neural networks and a sliding-mode based controller," *Smart Mater. Struct.*, vol. 12, pp. 223–231, 2003.
- [18] M. H. Elahinia, J. Koo, M. Ahmadian, and C. Woolsley, "Backstepping control of an SMA-actuated robotic arm," *J. Vib. Control*, vol. 11, no. 3, pp. 407–429, 2005.
- [19] S. W. Rhee and L. R. Koval, "Comparison of classical with robust control for SMA smart structures," *Smart Mater. Struct.*, vol. 2, pp. 162–171, 1993.
- [20] S. Choi and C. C. Cheong, "Vibration control of flexible beams using smart memory alloy actuators," *J. Guid. Control Dyn.*, vol. 19, pp. 1178–1180, 1996.
- [21] K. Tanaka, "A thermomechanical sketch of shape memory effect: One dimensional tensile behaviour," *Res. Mech.*, vol. 18, pp. 251–263, 1986.
- [22] C. Liang and C. A. Rogers, "One-dimensional thermomechanical constitutive relations of shape memory materials," *J. Intell. Mater. Syst. Struct.*, vol. 1, no. 2, pp. 207–234, 1990.
- [23] L. C. Brinson, "One-dimensionally constitutive behaviour of shape memory alloys: Thermomechanical derivation with non-constant material functions and redefined martensite internal variable," *J. Intell. Mater. Syst. Struct.*, vol. 4, no. 2, pp. 229–242, 1993.
- [24] M. H. Elahinia and M. Ahmadian, "An enhanced SMA phenomenological model: II. The experimental study," *Smart Mater. Struct.*, vol. 14, pp. 1309–1319, 2005.
- [25] H. K. Khalil, *Nonlinear Systems*, 3rd ed. Englewood Cliffs, NJ: Prentice Hall, 2001.
- [26] M. H. Elahinia and M. Ahmadian, "An enhanced SMA phenomenological model: I. The shortcomings of the existing models," *Smart Mater. Struct.*, vol. 14, pp. 1297–1308, 2005.



Shuzhi Sam Ge (S'90–M'92–SM'99–F'06) received the B.Sc. degree in control engineering from Beijing University of Aeronautics and Astronautics (BUAA), Beijing, China, and the Ph.D. degree in robotics and the Diploma of Imperial College from the Imperial College of Science, Technology and Medicine, University of London, London, U.K.

Currently, he is a Professor in the Department of Electrical and Computer Engineering, National University of Singapore, Singapore. He is the author or coauthor of more than 300 international journal and conference papers, and 3 books, *Adaptive Neural Network Control of Robotic Manipulators* (World Scientific, 1998), *Stable Adaptive Neural Network Control*

(Kluwer, 2001), and *Switched Linear Systems: Control and Design* (Springer-Verlag, 2005). His current research interests include robotics, adaptive control, hybrid systems, and intelligent multimedia fusion.

Dr. Ge is a Registered Professional Engineer. He is the recipient of the 1999 National Technology Award, the 2001 University Young Research Award, the 2002 Temasek Young Investigator Award, Singapore, and the 2004 Outstanding Overseas Young Researcher Award from the National Science Foundation, China. He is an Associate Editor of IEEE TRANSACTIONS ON AUTOMATIC CONTROL, IEEE TRANSACTIONS ON CONTROL SYSTEMS TECHNOLOGY, IEEE TRANSACTIONS ON NEURAL NETWORKS, and *Automatica*, and an Editor of *International Journal of Control, Automation and Systems*.



Keng Peng Tee (S'04) received the B.Eng. and M.Eng. degrees in mechanical engineering in 2001 and 2003, respectively, from the National University of Singapore, Singapore, where he is currently working toward the Ph.D. degree at the Department of Electrical and Computer Engineering.

His current research interests include intelligent and adaptive control with applications in mechatronic systems.



Ivan E. Vahhi received the B.Sc. degree in physics and the Ph.D. degree in physics and mathematics from St. Petersburg State Polytechnic University, St. Petersburg, Russia, in 1979 and 1990, respectively.

He is currently an Associate Professor at St. Petersburg State Polytechnic University. His current research interests include shape memory smart materials and their use in actuators and robotics.



Francis E. H. Tay received the B.Eng. and M.Eng. degrees from the National University of Singapore, Singapore, and the Ph.D. degree from Massachusetts Institute of Technology, Cambridge, in 1986, 1992, and 1996, respectively, all in mechanical engineering.

He has been a Technical Manager of the Micro and Nano Systems Cluster, Institute of Materials Research and Engineering. He is currently an Associate Professor in the Mechanical Engineering Department, National University of Singapore, Singapore. He is also a Group Leader of the Medical Devices Group, Institute of Bioengineering and Nanotechnology. His current research interests include biochip, wearable systems, and microfluidics.